Mon. Not. R. Astron. Soc. **369,** 249–256 (2006) doi:10.1111/j.1365-2966.2006.10298.x

High-eccentricity planets from the Anglo-Australian Planet Search

Hugh R. A. Jones,[1⋆] R. Paul Butler,[2] C. G. Tinney,[3] Geoffrey W. Marcy,[4] Brad D. Carter,[5] Alan J. Penny,[6,7] Chris McCarthy[8] and Jeremy Bailey[9]

[1]*Centre for Astrophysics Research, University of Hertfordshire, College Lane, Hatfield, Herts AL10 9AB* [2]*Carnegie Institution of Washington, Department of Terrestrial Magnetism, 5241 Broad Branch Rd NW, Washington, DC 20015-1305, USA* [3]*Anglo-Australian Observatory, PO Box 296, Epping 1710, Australia* [4]*Department of Astronomy, University of California, Berkeley, CA 94720, USA* [5]*Faculty of Sciences, University of Southern Queensland, Toowoomba, QLD 4350, Australia* [6]*Rutherford Appleton Laboratory, Chilton, Didcot, Oxon OX11 0QX* [7]*SETI Institute, 515 N. Whisman Road, Mountain View, CA 94043, USA* [8]*Department of Physics and Astronomy, San Francisco State University, San Francisco, CA 94132, USA* [9]*Australian Centre for Astrobiology, Macquarie University, Sydney, NSW 2109, Australia*

Accepted 2006 March 6. Received 2006 March 4; in original form 2005 October 26

ABSTRACT

We report Doppler measurements of the stars HD 187085 and HD 20782 which indicate two high eccentricity low-mass companions to the stars. We find HD 187085 has a Jupiter-mass companion with a ∼1000-d orbit. Our formal 'best-fitting' solution suggests an eccentricity of 0.47, however, it does not sample the periastron passage of the companion and we find that orbital solutions with eccentricities between 0.1 and 0.8 give only slightly poorer fits (based on rms and χ^2_ν) and are thus plausible. Observations made during periastron passage in 2007 June should allow for the reliable determination of the orbital eccentricity for the companion to HD 187085. Our data set for HD 20782 does sample periastron and so the orbit for its companion can be more reliably determined. We find the companion to HD 20782 has M sin $i = 1.77 \pm 0.22\, M_{\rm Jup}$, an orbital period of 595.86 ± 0.03 d and an orbit with an eccentricity of 0.92 ± 0.03. The detection of such high-eccentricity (and relatively low-velocity amplitude) exoplanets appears to be facilitated by the long-term precision of the Anglo-Australian Planet Search. Looking at exoplanet detections as a whole, we find that those with higher eccentricity seem to have relatively higher velocity amplitudes indicating higher mass planets and/or an observational bias against the detection of high-eccentricity systems.

Key words: stars: individual: HD 187085 – stars: individual: HD 20782 – stars: brown dwarfs – planetary systems.

1 INTRODUCTION

The Anglo-Australian Planet Search (AAPS) is a long-term radial velocity (RV) project engaged in the detection and measurement of extrasolar planets (hereafter, shortened to exoplanets) at the highest possible precisions. Together with programmes using similar techniques on the Lick 3-m and Keck I 10-m telescopes (Butler & Marcy 1997; Vogt et al. 2000), it provides all-sky planet search coverage for inactive F, G, K and M dwarfs down to a magnitude limit of $V = 7.5$. So far the AAPS has has published data for 23 exoplanets (Butler et al. 2001; Tinney et al. 2001, 2002a, 2003, 2005, 2006; Jones et al. 2002a,b, 2003; Carter et al. 2003; McCarthy et al. 2005) as well as non-detections of planets claimed elsewhere (Butler et al. 2001, 2002).

The AAPS is carried out on the 3.9-m Anglo-Australian Telescope (AAT) using the University College London Echelle Spectrograph (UCLES), operated in its 31 lines mm^{-1} mode together with an I_2 absorption cell. UCLES now uses the AAO's EEV 2048 × 4096 13.5-μm pixel CCD, which provides excellent quantum efficiency across the 500–620 nm I_2 absorption line region. From 1998 until 2002, the AAPS allocation was around 20 nights per year, from 2002 to 2004 it increased to 32. In 2005, the AAPS has an allocation of 64 nights per year. Despite this search taking place on a common-user telescope with frequent changes of instrument, we have historically achieved a 3 m s^{-1} precision down to the $V = 7.5$ mag limit of the survey (e.g. fig. 1, Jones et al. 2002a), for stars with low 'jitter'. In addition to our published errors, there are additional sources of error collectively termed 'jitter'. The magnitude of the 'jitter' is a function of the spectral type of the star observed. Wright (2005) gives a model which estimates the jitter for a star based upon its activity. Our continuing attainment of 3 m s^{-1} single-shot precision for suitably inactive stars is demonstrated in McCarthy et al. (2004) and Tinney et al. (2005).

Our target sample, which we have observed since 1998, is given

⋆E-mail: hraj@star.herts.ac.uk

in Jones et al. (2002b). It includes 178 late (IV-V) F, G and K stars with declinations below $\sim -20^\circ$ and is complete to $V < 7.5$. We also observe subsamples of 20 metal-rich ([Fe/H] > 0.3) stars with $V < 9.5$ and 7 M dwarfs with $V < 11$ and declinations below $\sim -20^\circ$. The sample has been increased to more than 250 solar-type stars to be complete to a magnitude limit of $V = 8$. Where age/activity information is available from $\log R'_{\rm HK}$ indices (Henry et al. 1996; Tinney et al. 2002b; Jenkins et al. 2006), we require target stars to have $\log R'_{\rm HK} < -4.5$ corresponding to ages typically greater than 3 Gyr. Stars with known stellar companions within 2 arcsec are removed from the observing list, as it is operationally difficult to get an uncontaminated spectrum of a star with a nearby companion. Spectroscopic binaries discovered during the programme have also been removed and are reported elsewhere (Blundell et al. 2006). Otherwise there is no bias against observing multiple stars. The programme is also not expected to have any bias against brown dwarf companions.

The observing and data processing procedures follow those described by Butler et al. (1996, 2001) and Tinney et al. (2005). All data taken by the AAPS to date have been reprocessed through our continuously upgraded analysis system. Here, we report results from the current version of our pipeline.

2 STELLAR CHARACTERISTICS OF HD 187085 AND HD 20782

The characteristics for HD 187085 and HD 20782 are summarized in Table 1. Houk (1982) assigns spectral types of G0V and G3V to HD 187085 and HD 20782 which are consistent with information derived for and from the Hipparcos mission (ESA 1997). Both stars have been included in large-scale studies of nearby solar-type stars. Nordstrom et al. (2004) included them in a magnitude-limited, kinematically unbiased study of 16682 nearby F and G dwarf stars. Valenti & Fischer (2005) included them in a study of the stellar properties for 1040 F, G and K stars observed for the Anglo-Australian, Lick and Keck planet search programmes. Valenti & Fischer used high signal-to-noise echelle spectra originally taken for template RV spectra and spectral synthesis to derive effective temperatures, surface gravities and metallicities, whereas Nordstrom et al. (2004) used Strömgren photometry and the infrared flux method calibration of Alonso, Arribas & Martinez-Roger (1996). Both studies use Hipparcos parallaxes to convert luminosities in order to make comparisons with different theoretical isochrones to derive stellar parameters. To determine, stellar masses and ages Valenti & Fischer, use Yonsei–Yale isochrones (Demarque, Woo & Kim 2004) and Nordstrom et al. (2004) use Padova isochrones (Giradri et al. 2000; Salasnich et al. 2000). Both sets of derived parameters agree to within errors.

Table 1. The stellar parameters for HD 187085 and HD 20782 tabulated below are taken from a range of sources: spectral types from Houk (1982); activities from Henry et al. (1996) and Tinney et al. (2002b); Hipparcos measurements from (ESA 1997); luminosities, masses, temperatures, metallicities and space velocities from Nordstrom et al. (2004, abbreviated as N04 in the table, the errors given for Nordstrom et al. values are the average of dispersions, no upper confidence limit is given for the age of HD 20782 by Nordstrom et al.) and Fischer & Valenti (2005, abbreviated as FV05 in the table); jitter values are taken from Wright (2005).

Parameter	HD 187085	HD 20782
Spectral type	G0V	G3V
$\log R'_{\rm HK}$	-4.93	-4.91
Hipparcos $N_{\rm obs}$	113	191
Hipparcos σ	0.0013	0.0009
$\log (L_{\rm star}/{\rm L}_\odot)$	$2.13 \pm {}^{0.55}_{0.44}$	$1.25 \pm {}^{0.2}_{0.17}$
$M_{\rm star}/{\rm M}_\odot$ – N04	$1.16 \pm {}^{0.06}_{0.08}$	$0.90 \pm {}^{0.07}_{0.03}$
$M_{\rm star}/{\rm M}_\odot$ – VF05	$1.22 \pm {}^{0.1}_{0.06}$	1.0 ± 0.03
$T_{\rm eff}$ (K) – N04	6011 ± 76	5636 ± 76
$T_{\rm eff}$ (K) – VF05	6075 ± 30	5758 ± 30
[Fe/H] – N04	0.05 ± 0.10	-0.16 ± 0.10
[Fe/H] – VF05	0.05 ± 0.03	-0.05 ± 0.03
U, V, W – N04 (km s^{-1})	11, -20, -14	-38, -61, -2
Age (Gyr) – N04	$3.9 \pm {}^{2.2}_{1.4}$	$13.0_{-4.5}$
Age (Gyr) – VF05	$3.3 \pm {}^{0.6}_{1.2}$	$7.1 \pm {}^{1.9}_{4.3}$
Jitter (m s^{-1})	2.80	4.11

Both HD 187085 and HD 20782 have moderate activity indices $\log R'_{\rm HK} \sim -4.9$ from Henry et al. (1996). For the case of HD 187085, we also have a confirmation measurement from our own CaHK programme (Fig. 1 and Tinney et al. 2002b) Furthermore, there is no evidence for significant photometric variability for either star in measurements made by the Hipparcos satellite. Combining Hipparcos astrometry with their RVs, Nordstrom et al. (2004) determine U, V, W space velocities. Based on Edvardsson et al. (1993) these ages are consistent with the derived ages in Table 1.

3 ORBITAL SOLUTION FOR HD 187085

The 40 epochs of Doppler velocity measurements for HD 187085, obtained between 1998 November and 2005 October, are shown graphically in Fig. 3 and listed in Table 2. Our velocity measurements are derived by breaking the spectra into several hundred 2-Å chunks and deriving velocities for each chunk. The velocity error, given in the third column and labelled 'error', is determined from the scatter of these chunks. This error includes the effects of photon-counting uncertainties, residual errors in the spectrograph point spread function (PSF) model and variation in the underlying spectrum between the template and iodine epochs. All velocities are measured relative to the zero-point defined by the template observation. Our periodogram analysis in Fig. 2 reveals a single broad peak around 1000 d at about the 0.05 per cent false alarm level and well above the indicated 1 per cent false alarm rate.

Our best-fitting solution yields an orbital period of 986 d, a semi-amplitude of stellar reflex motion (which we shorten to velocity

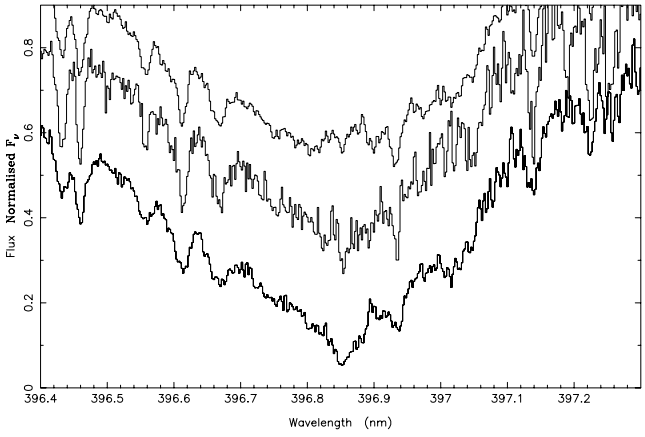

Figure 1. UCLES spectrum of the region of the CaHK line for HD 20782 (middle, $\log R'_{\rm HK} = -4.93$, G3V) and two comparison objects of similar spectral types and activities HD 17051 (top, $\log R'_{\rm HK} = -4.81$, G0V) and HD 142 (bottom, $\log R'_{\rm HK} = -4.95$, G0V). The spectra are taken from Tinney et al. (2002b).

Table 2. Relative RVs are given for HD 187085. JD are heliocentric. RVs are barycentric but have an arbitrary zero-point determined by the RV of the template.

JD (-245 1000)	RV ($m\,s^{-1}$)	Error ($m\,s^{-1}$)
120.9170	−12.1	5.3
411.0753	−2.5	6.5
683.1693	16.1	5.7
743.0494	9.3	5.5
767.0046	8.8	4.7
769.0652	5.3	4.4
770.1153	5.3	5.2
855.9477	8.6	8.9
1061.2140	−4.5	5.3
1092.0512	−28.2	5.9
1128.0267	−25.9	5.1
1151.0146	−15.4	6.8
1189.9230	−6.4	4.2
1360.2816	−7.3	4.6
1387.2168	−8.7	3.5
1388.2355	−12.1	3.7
1389.2664	−12.9	4.3
1422.2121	−6.9	4.0
1456.0917	−7.9	4.9
1750.2587	13.5	3.8
1752.2311	11.9	3.8
1784.2071	19.6	3.2
1857.1218	−4.2	3.7
1861.0168	9.2	4.5
1942.9842	17.2	4.2
1946.9260	17.9	3.2
2217.0666	−12.1	3.7
2245.0429	−24.0	5.9
2484.3002	−3.0	3.7
2489.2600	−5.2	3.4
2507.1966	−0.7	2.8
2510.2154	−2.1	3.3
2517.2619	−3.5	4.1
2520.2747	−10.4	4.2
2569.0854	−5.8	3.9
2572.1667	−8.3	4.5
2577.0269	2.1	3.0
2627.9629	9.8	5.8
2632.0744	6.7	3.4
2665.9534	18.9	3.7

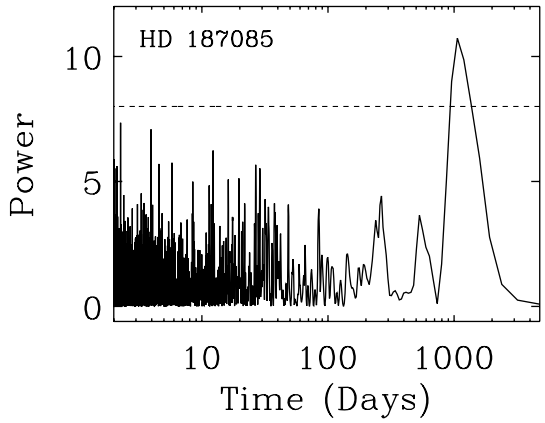

Figure 2. A periodogram of the 40 epochs of HD 187085 obtained at the AAT between 1998 November and 2005 October. The false alarm probabilities shown are based on the assumption of normally distributed errors. The dashed line is the 1 per cent false alarm level.

amplitude) of $17\,m\,s^{-1}$, and an eccentricity of 0.47. The fit is shown in the upper part of Fig. 3. The rms to the Keplerian fit is $7.07\,m\,s^{-1}$, yielding a χ^2_ν of 1.82. This solution implies a minimum (M sin i) mass of 0.75 $M_{\rm Jup}$, and a semimajor axis of 2.05 au. However, the Keplerian curve of this eccentric orbit includes both a peak and a sharp drop that are not sampled by our velocities. This raises the possibility that an orbit of lower eccentricity might fit the data nearly as well. Orbits with lower eccentricity deserve consideration because of the lower effective degrees of freedom harboured by such orbits. We tried other orbital solutions with fixed eccentricities. We find a wide range of eccentricities fit the data. For example, a fixed eccentricity of 0.1 yields the same value of rms (shown in the lower part of Fig. 3). This is consistent with the numerical simulations reported in Butler et al. (2004) which indicate the uncertainty in determining eccentricity becomes large for low-amplitude signals. The next periastron passage for HD187085 is 2007 June at which time the eccentricity solution can be better constrained.

Based on associating an object with others that reside near it on an HR diagram and finding the best-fitting relationship between observed jitter and activity, Wright (2005) predict a jitter of $2.8\,m\,s^{-1}$ for HD 187085. Combining the expected error of $3\,m\,s^{-1}$ in quadrature with the expected jitter error the expected rms error of $4.25\,m\,s^{-1}$ is rather lower than our plausible orbital solutions which have $\sim 7\,m\,s^{-1}$ rms. We expect these higher rms values arise because the stellar jitter relationship for inactive stars is relatively poorly determined and also because our precision for HD 187085 is limited by the slightly smaller equivalent widths of its stellar lines relative to later spectral types. Thus with our observing exposures adjusted to give signal-to-noise = 200 per exposure our precision is probably limited to around $4\,m\,s^{-1}$ rather than $3\,m\,s^{-1}$. The lack of any observed variation in chromospheric activity between Henry et al. (1996) and Tinney et al. (2002b) or significant photometric variability within the Hipparcos data set gives us confidence that the Keplerian curve arises from an exoplanet rather than from long-period star-spots or chromospherically active regions.

4 ORBITAL SOLUTION FOR HD 20782

The 29 epochs of Doppler measurements for HD 20782, obtained between 1998 August and 2005 September, are shown graphically in Fig. 4 and listed in Table 3. For cases of extreme eccentricity, like HD 20782, periodograms break down. The best-fitting orbit is found by searching over a wide-swath of period space. In the case of HD 20782 this is simplified by the large velocity amplitude of the velocity variations.

The data are well fit by a Keplerian curve which yields an orbital period of 585.86 ± 0.03 d, a velocity amplitude of $115 \pm 12\,m\,s^{-1}$ and an eccentricity of 0.92 ± 0.03. The minimum (M sin i) mass of the planet is $1.77 \pm 0.22\,M_{\rm Jup}$ and the semimajor axis is 2.26 ± 0.46 au. The rms to the Keplerian fit is $5.0\,m\,s^{-1}$, yielding a reduced χ^2_ν of 1.01. Wright (2005) predicts a jitter of $4.1\,m\,s^{-1}$. Our errors come from Monte Carlo simulations where the best-fitting Keplerian orbit is recomputed based on the noise in the data. Combining our

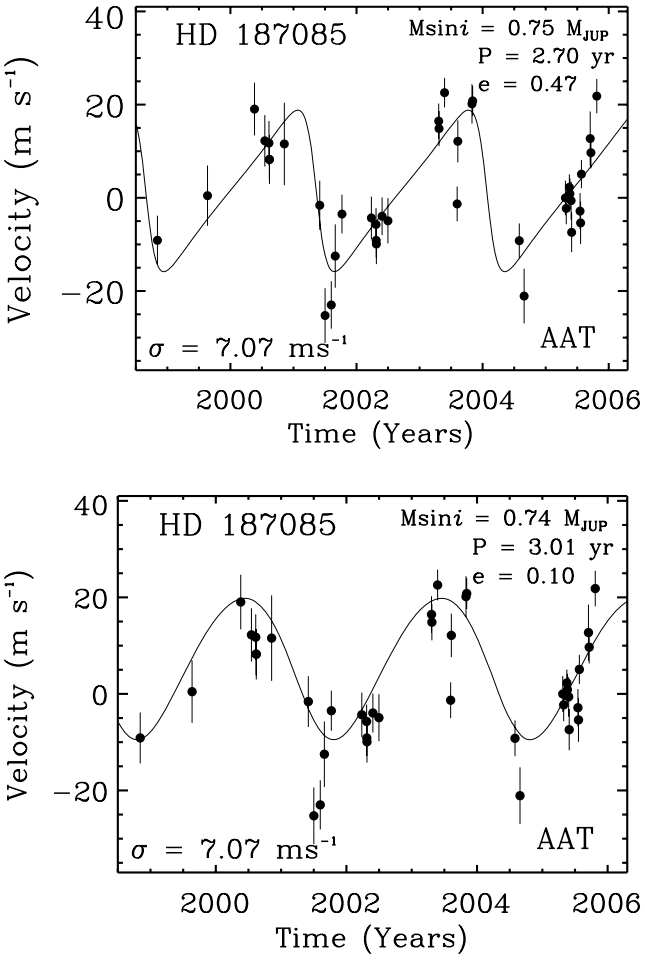

Figure 3. Doppler velocities obtained for HD 187085 from 1998 August to 2005 October. The top plot shows the best-fitting eccentricity, the bottom plot shows a similar quality fit for a fixed eccentricity of 0.1. In both cases the solid lines indicate the best-fitting Keplerian with the parameters shown.

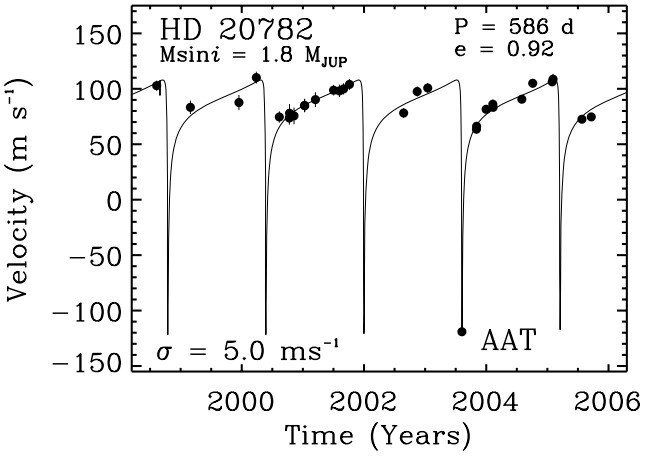

Figure 4. Doppler velocities obtained for HD 20782 from 1998 August to 2005 September. The solid line is a best-fitting Keplerian with the parameters shown in Table 4. The rms of the velocities about the fit is 5.0 m s^{-1}. Based on a primary mass of 0.95 $M_\odot$, the minimum (M sin i) mass of the companion is 1.77 $M_{\rm Jup}$ and the semimajor axis is 1.36 au.

expected error of 3 m s^{-1} in quadrature with the expected jitter gives an expected rms of 5.1 m s^{-1}, consistent with the measured value. Furthermore, the lack of any observed chromospheric activity or photometric variations gives us confidence that the Keplerian curve arises from an exoplanet rather than from long-period star-spots or chromospherically active regions. The properties of the candidate exoplanet in orbit around HD 20782 are summarized in Table 4.

While we are confident about our procedures and the consistency of our solution, we find that within our errors HD 20782 shares the status of 'most highly eccentric exoplanet' along with HD 80606 (e = 0.9330 ± 0.0067, Butler et al. 2006; e = 0.927 ± 0.012, Naef et al. 2001). Thus it is important that we examine the reality and our reliance on our single periastron data point (Julian Dates (JD) 245 1000 = 1859.3054, RV = −197.6 m s^{-1}). If the time of this epoch were recorded wrong by about 3 h, the barycentric correction would be off by about 200 m s^{-1} due to diurnal rotation. A check of the continuity of the logsheets rules this out and reveals that the periastron observations were taken under a clear sky. However, if the star were by chance observed near the Moon or in twilight the G2V reflected solar spectrum might drag the spectral line centroid off.

At the time of observation the Moon as seen from Siding Spring was at $17^{\rm h}03^{\rm m}32^{\rm s}$ − 23°59′57″ (J2000 – from the JPL Horizons System, http://ssd.jpl.nasa.gov/horizons.html). HD 20782 is at $03^{\rm h}20^{\rm m}04^{\rm s}$ − 28°51′15″ (J2000). Thus HD 20782 was nowhere near the Moon. In fact, the star is well off the ecliptic so can never get very close to the Moon. The observation time (the mid-point of the exposure) was 4 min before the start of morning −18° (astronomical) twilight. At this time there should be no significant twilight contamination in the two 10-min exposures taken of HD 20782, indeed AAPS observations routinely continue until −12° twilight. We are reassured of our strategy because based on our test exposures with UCLES looking at blank sky 20 min after −12° twilight no sky photons are detected in a 1-min exposure (above read noise). Any solar contamination would generate a high χ^2_ν statistic for the quality of the doppler fit. The formal internal errors for the two observations, made consecutively at the periastron epoch, were 5.1 and 5.5 m s^{-1}, compared with a median of 5.3 m s^{-1} for all observations of HD 20782. So, the individual spectra making up our periastron data point show no extra scatter in velocity.

Despite our confidence in these two data points comprising the JD 245 000 = 1859.3054 epoch we also recomputed the Keplerian fit after removing them from the data set. The resulting best-fitting parameters are period = 599.82 d, periastron time (JD) = 51 067.098, eccentricity = 0.732, ω = 119.6°, velocity amplitude = 32.7 m s^{-1} and planetary mass = 0.92 $M_{\rm Jup}$. With this new fit the period is the same as before, but the values of eccentricity and velocity amplitude (and thus planetary mass) are significantly lower. So, although the qualitative sense of the orbit remains nearly the same, the epoch of low-velocity data do force the velocity amplitude, eccentricity and planetary mass to be smaller than if we didn't have them. Thus, while we are confident of the extreme eccentricity of HD 20782b, we would like to obtain further data points near periastron. At the last periastron (2005 March 27) we were unable to observe HD 20782. The constrained blocks of time awarded to the AAPS restricts our ability to reactively schedule time-critical observations such as those we wish to make for HD 20782.

5 DISCUSSION

The two exoplanets presented here have relatively large eccentricities and small velocity amplitudes. With an eccentricity of

Table 3. Relative RVs are given for HD 20782. JD are heliocentric. RVs are barycentric but have an arbitrary zero-point determined by the RV of the template.

JD (-245 1000)	RV ($m\,s^{-1}$)	Error ($m\,s^{-1}$)
35.3195	24.3	4.6
236.9306	4.8	6.0
527.0173	9.2	6.8
630.8824	31.7	5.3
768.3089	−3.9	5.1
828.1107	−4.8	6.0
829.2745	−0.5	8.3
856.1353	−2.9	7.5
919.0066	6.5	6.1
919.9963	6.3	5.7
983.8901	11.8	6.6
1092.3044	20.3	4.7
1127.2681	19.6	5.6
1152.1631	21.4	5.1
1187.1597	25.5	4.9
1511.2066	−0.3	4.5
1592.0484	19.1	4.5
1654.9603	22.3	4.4
1859.3054	−197.6	3.8
1946.1383	−14.9	4.0
1947.1225	−12.3	3.4
2004.0015	3.1	3.6
2044.0237	7.6	4.3
2045.9607	4.8	3.8
2217.2881	12.1	3.3
2282.2204	26.5	3.8
2398.9697	27.8	2.6
2403.9607	30.3	4.8
2576.3073	−5.9	3.0
2632.2813	−3.8	3.2

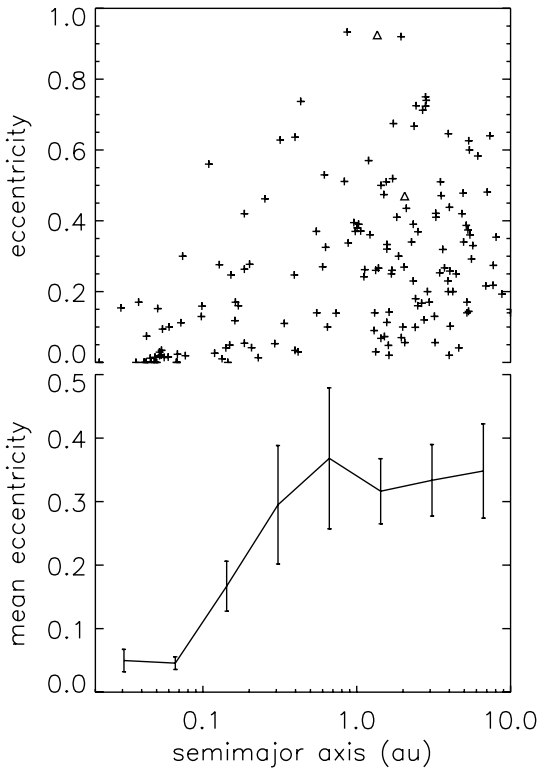

Figure 5. The upper plot shows a scatter plot for eccentricities against semimajor axis for exoplanets, within 200 pc, with semimajor axes <10 au and masses less than 20 $M_{\rm Jup}$ as given by table 2 of Butler et al. (2006). The values for the candidate exoplanets presented here are shown as triangles. The lower plot shows mean eccentricities plotted against semimajor axis for exoplanets. Tidal circularization dominates the close-in planets with eccentricities reaching a plateau by around 0.2 au. The error bars are from $\sqrt{(\text{number})}$ statistics and are only indicative. The plots show results from many surveys and are thus drawn from an inhomogeneous sample.

Table 4. Orbital parameters for the companions to HD 187085 and HD 20782.

Parameter	HD 187085	HD 20782
Orbital period P (d)	986	585.86 ± 0.03
Velocity amplitude K ($m\,s^{-1}$)	17	115 ± 12
Eccentricity e	0.47	0.92 ± 0.03
ω (°)	94	147 ± 3
Periastron time (JD)	245 0912	$245\,1687.1 \pm 2.5$
$M \sin i$ ($M_{\rm Jup}$)	0.75	1.80 ± 0.23
Semimajor axis a (au)	2.05	1.36 ± 0.12
rms ($m\,s^{-1}$)	7.1	5.0

0.925 ± 0.030, HD 20782 has a comparable eccentricity to HD 80606 ($e = 0.9330 \pm 0.0067$, Butler et al. 2006; $e = 0.927 \pm 0.012$, Naef et al. 2001) which has the highest value of eccentricity reported to date. The companion to HD 187085 has a more modest and uncertain eccentricity. Nonetheless its combination of large eccentricity and small velocity amplitude make it noteworthy. It may have one of the highest known eccentricities, alternatively, low-eccentricity fits yield velocity amplitude solutions less than $15\,m\,s^{-1}$ making it one of only a handful of low-velocity amplitude, long-period exoplanet detections. On the other hand, if a low value of eccentricity is appropriate for the orbital solution of HD 187085 then velocity amplitude solutions of less than $15\,m\,s^{-1}$ will be fit placing the companion to HD 187085 with only a handful of low-velocity amplitude, long-period exoplanet detections.

The relative rarity of such high-eccentricity planets can be seen in Fig. 5. The plot shows a clear deficit of eccentric planets with small semimajor axes. For planets with periastron distances less than 0.1 au this deficit is expected (e.g. Rasio & Ford 1996) and seen to be due to the tidal circularization of close-in planets (e.g. Halbwachs, Mayor & Udry 2005). However, for periastron distances of 0.1 au the tidal circularization time-scale is already likely to be many Gyr, for inferred Q values (based on planets having semimajor axes with less than 0.1 au, where Q is the specific dissipation function). The circularization time-scale, $t_{\rm circ}$, is a sensitive function of the radius of the planet, $R_{\rm planet}$ ($t_{\rm circ} \propto R_{\rm planet}^{-5}$, Goldreich & Soter 1966) and supposedly occurs due to dissipation in the planet, not the star (e.g. Gu, Bodenheimer & Lin 2004). Perhaps, the larger planet radii during contraction, in the first 10 Myr or so, helps to shorten the circularization time. Thus the rising mean eccentricities versus semimajor axis apparent in Fig. 5 from 0.1 to 0.3 au may be explained by the decreasing effectiveness of the tidal circularization mechanism.

Fig. 5, in particular the lower binned plot, indicates that mean eccentricities rise steeply reaching a plateau beyond around 0.3 au. Thereafter, the eccentricity of an exoplanet appears roughly

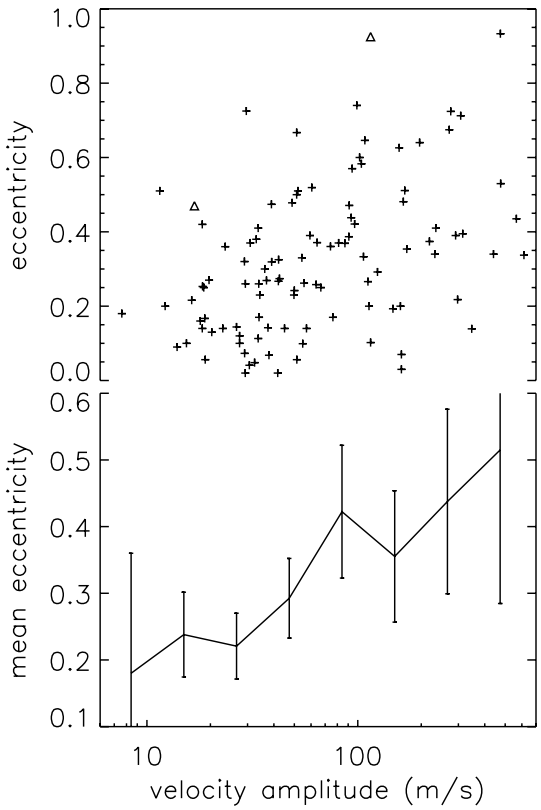

Figure 6. The upper plot shows a scatter plot for eccentricities against velocity amplitude for exoplanets, within 200 pc, with semimajor axes 0.5–10 au and masses less than 20 $M_{\rm Jup}$ as given by table 2 of Butler et al. (2006). The values for the exoplanets. The lower plot shows mean eccentricities plotted against velocity amplitudes. The error bars are $\sqrt{\text{(number)}}$ statistics and are only indicative. The plots show results from many surveys and are thus drawn from an inhomogeneous sample.

constant. Beyond 2 au there may be a slight deficit of high-eccentricity exoplanets apparent from the lack of objects in the top right of the upper part of Fig. 5. In order to detect highly eccentric exoplanets with long periods, it is necessary to have good time sampling. For example, the detection of the ultrasharp periastron passages of eccentric orbits requires relatively large numbers of observations as well as fortitous sampling. In the case of HD 20782, we only have one epoch near periastron passage. Nonetheless, our robust observing and data reduction procedures and the relatively large (115 m s^{-1}) amplitude signal gives us confidence that we have detected a high-eccentricity orbit. Cumming (2004) illustrates the difficulties of detecting planets of high eccentricities with limited sampling. His work shows that even with high signal-to-noise and representative numbers of data points, 'there remain significant selection effects against eccentric orbits for $e > 0.6$'.

While time sampling is crucial for adequate sampling of highly eccentric orbits, it is also appropriate to comment on precision. The top left of Fig. 6 is relatively poorly populated. As discussed above this is likely to be due to difficulties associated with the detection of high-eccentricity orbits. In addition, there maybe a relatively smaller population of high-eccentricity exoplanets. However, at more modest eccentrcities, there is an apparent deficit of low-velocity amplitude exoplanets. It is interesting to look at the objects that define the upper envelope of the top left of the upper part of Fig. 6. These objects represent the highest eccentricity objects that have been found for a given velocity amplitude. In addition to the companion to HD 20782 reported here, the other two objects are HD 45350b (Marcy et al. 2005a) and HD 11964b (Butler et al. 2006), both recently discovered using Keck data. Both the AAPS and Keck planet search operate with demonstrated long-term precisions of around 3 m s^{-1} (e.g. fig. 1, Tinney et al. 2005 and fig, 2, Vogt et al. 2005). Such long-term precisions may now be rivalled over shorter baselines by the HARPS (e.g. Lovis et al. 2005) and Hobby–Eberly (e.g. McArthur et al. 2004) planet search projects though many of the objects plotted in Fig. 6 were discovered by searches with lesser long-term precision. While the importance of precision is widely recognized its specific importance for the detection of high eccentricities has been anticipated in the simulations of Cumming (2004) and Halbwachs et al. (2005). Cumming's fig. 4 shows that the detectability of exoplanets with $e > 0.7$ is a function of precision. Thus, simulations and the exoplanets detected so far serve to suggest that RVs with good long-term precision are important to robustly sample the parameter space occupied by highly eccentric planets.

The observational difficulties inherent in the detection of low-velocity amplitude – high-eccentricity planets predicted by Cumming and suggested in the upper part of Fig. 6 appear to be borne out by the binned (lower part) of the figure. These binned data suggest that the velocity amplitude of exoplanets increases with mean eccentricity in Fig. 6, albeit with low confidence since it is almost possible to draw a flat line through all the error bars. While we have attempted to remove the effects of circularization processes from Fig. 6 (by removing all planets with semimajor axes less than 0.5 au), it is plausible that the suggested trend may have a physical origin. In particular, it is notable that beyond the tidal circularization limit (usually assumed to be 0.1 au) spectroscopic binaries have significantly higher eccentricities than exoplanets (Halbwachs et al. 2005) and that high-mass planets (also having high-velocity amplitudes) have systematically higher eccentricities than low-mass planets, e.g. 70 Vir (Marcy & Butler 1996) and fig. 5, Marcy et al. (2005b). Fig. 7 shows this correlation of eccentricity with mass for the exoplanet sample of Butler et al. (2006). For large velocity amplitudes and large mass planets this cannot be a selection effect nor can it be caused by errors because the most massive planets induce the largest Keplerian amplitudes, allowing precise determination of eccentricity. To quantify the reality of the suggested trends, to assess observational bias at high eccentricities and to recover the underlying eccentricity distribution of exoplanets analysis of the RV data for each different survey is required. Such work has been started by Cumming, Marcy & Butler (1999) and Cumming et al. (2003) and independently by the Anglo-Australian Planet Search.

By the standards of our Solar system, the majority of exoplanets beyond 1 au can be seen from Fig. 5 to be in eccentric orbits. This contrast with the Solar system may be at least partly explained by as yet unseen long-period companions. Indeed the fits for a few of the long-period eccentric planets do already include longer period trends though these are generally rather modest and sometimes uncertain, e.g. our 'best-fitting' solution for HD 187085 includes an additional slope of 1.3 ± 1.0 m s^{-1}. So while individual cases require careful consideration, the lack of substantial trends in the current sample of high-eccentricty exoplanets (e.g. Butler et al. 2006) means that the majority of the observed eccentricities need to be explained by high-formation eccentricties or by appropriate eccentricity pumping mechanisms. Since the derived masses of exoplanets are directly proportional to measured velocity amplitude it is important to account for the likely observational eccentricity bias when investigating mass dependencies of exoplanets and in particular when trying to understand the relative importance of different

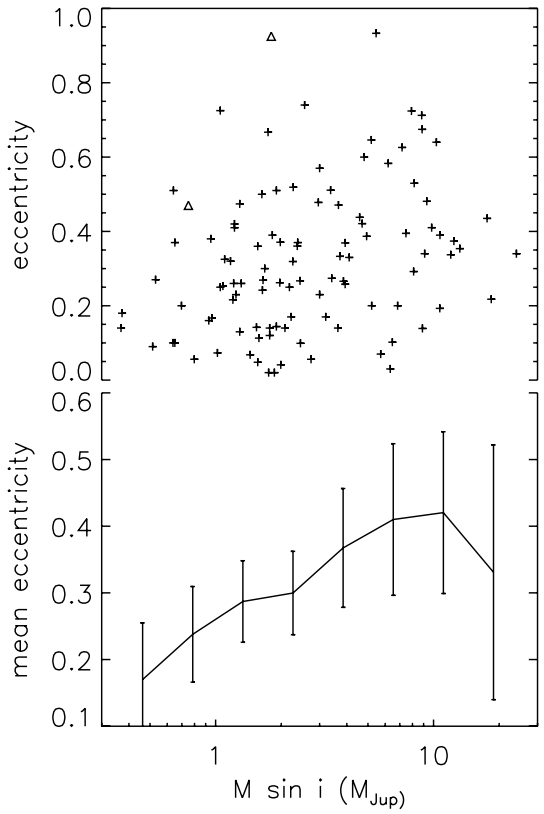

Figure 7. The upper plot shows a scatter plot for eccentricities against $M \sin i\, M_{\rm Jup}$ for exoplanets within 200 pc with semimajor axes 0.5–10 au and masses less than 20 $M_{\rm Jup}$ as given by table 2 of Butler et al. (2006). The values for the exoplanets presented here are shown as triangles. The error bars are $\sqrt{(\text{number})}$ statistics and are only indicative. The plots show results from many surveys and are thus drawn from an inhomogeneous sample.

eccentricity pumping mechanisms (e.g. Takeda & Rasio 2005). We are encouraged to proceed in earnest with our project to examine the detectability of Anglo-Australian Planet Search exoplanets of different eccentricities (and other parameters), given our errors and time sampling. This should improve our search and will put us in a better position to better understand the underlying distribution of eccentricity with mass and semimajor axis for exoplanets.

ACKNOWLEDGMENTS

We thank the referee Gordon Walker for his valuable comments. We are very grateful for the support of the Director of the AAO, Dr Matthew Colless, and the superb technical support which has been received throughout the programme from AAT staff – in particular John Collins, Shaun James, Steve Lee, Rob Patterson, Jonathan Pogson and Darren Stafford. We gratefully acknowledge the UK and Australian government support of the Anglo-Australian Telescope through their PPARC and DETYA funding (HRAJ, AJP, CGT); NASA grant NAG5-8299 and NSF grant AST95-20443 (GWM); NSF grant AST-9988087 (RPB); and Sun Microsystems. This research has made use of the SIMBAD data base, operated at CDS, Strasbourg, France.

REFERENCES

Alonso A., Arribas S., Martinez-Roger C., 1996, A&A, 313, 873
Blundell J. et al., 2006, MNRAS, submitted
Butler R. P., Marcy G. W., 1997, in Cosmovici C. S., Bowyer S., Werthimer D., eds, Proc. IAU Colloq. 161, Astronomical and Biochemical Origins and the Search for Life in the Universe. Warsaw Technical University, Warsaw, p. 331
Butler R. P., Marcy G. W., Williams E., McCarthy C., Dosanjh P., Vogt S. S., 1996, PASP, 108, 500
Butler R. P., Tinney C. G., Marcy G. W., Jones H. R. A., Penny A. J., Apps K., 2001, ApJ, 555, 410
Butler R. P., Marcy G. W., Fischer D. A., Vogt S. S., Tinney C. G., Jones H. R. A., Penny A. J., Apps K., 2004, in Penny A., Artymowicz P., Lagrange A.-M., Russell S., eds, IAU Symp. 202, Planetary Systems in the Universe: Observations, Formation and Evolution. Astron. Soc. Pac., San Francisco, p. 3
Butler R. P. et al., 2002, ApJ, 578, 565
Butler R. P. et al., 2006, ApJ, in press
Carter B. D., Butler R. P., Tinney C. G., Jones H. R. A., Marcy G. W., Fischer D. A., Penny A. J., 2003, ApJ, 593, L43
Cumming A., 2004, MNRAS, 354, 1165
Cumming A., Marcy G. W., Butler R. P., 1999, ApJ, 526, 896
Cumming A., Marcy G. W., Butler R. P., Vogt S. S., 2003, in Deming D., Seager S., eds, ASP Conf. Ser. Vol. 294, Scientific Frontiers in Research on Extrasolar Planets. Astron. Soc. Pac., San Francisco, p. 27
Demarque P., Woo J.-H., Kim Y.-Yi S., 2004, ApJS, 155, 667
Edvardsson B., Andersen J., Gustafsson B., Lambert D. L., Nissen P. E., Tomkin J., 1993, A&A, 275, 101
ESA, 1997, The HIPPARCOS and Tycho Catalogues, ESA SP-1200
Fischer D. A., Valenti J., 2005, ApJ, 622, 1102 (FV05)
Giradri L., Bressan A., Bertelli G., Chiosi C., 2000, A&AS, 141, 371
Goldreich P., Soter S., 1966, Icarus, 5, 375
Gu P.-G., Bodenheimer P. H., Lin D. N. C., 2004, ApJ, 608, 1076
Halbwachs J. L., Mayor M., Udry S., 2005, A&A, 431, 1129
Henry T. J., Soderblom D. R., Donahue R. A., Baliunas S. L., 1996, AJ, 111, 439
Houk N., 1982, Catalogue of Two-Dimensional Spectral Types for the HD Stars, Vol. 3. Department of Astronomy, University of Michigan, University Microfilms International, Ann Arbor, MI
Jenkins J. S., Jones H. R. A., Tinney C. G., Butler R. P., Marcy G. W., McCarthy C., Carter B. D., Penny A. J., 2006, MNRAS, submitted
Jones H. R. A., Butler R. P., Tinney C. G., Marcy G. W., Penny A. J., McCarthy C., Carter B. D., Pourbaix D., 2002a, MNRAS, 333, 871
Jones H. R. A., Butler R. P., Tinney C. G., Marcy G. W., Penny A. J., McCarthy C., Carter B. D., 2002b, MNRAS, 337, 1170
Jones H. R. A., Butler R. P., Tinney C. G., Marcy G. W., Penny A. J., McCarthy C., Carter B. D., 2003, MNRAS, 341, 948
Lovis C. et al., 2005, A&A, 437, 1121
Marcy G. W., Butler R. P., 1996, ApJ, 464, L147
Marcy G. W., Butler R. P., Fischer D. A., Vogt S. S., 2005a, ApJ, 619, 570
Marcy G. W., Butler R. P., Fischer D. A., Vogt S. S., Wright J. T., Tinney C. G., Jones H. R. A., 2005b, Prog. Theor. Phys. Suppl., 158, 24
McArthur B. et al., 2004, ApJ, 614, 81
McCarthy C., Butler R. P., Tinney C. G., Jones H. R. A., Marcy G. W., Carter B. D., Penny A. J., Fischer D., 2004, ApJ, 617, 575
Naef D. et al., 2001, A&A, 375, 27
Nordstrom B. et al., 2004, A&A, 418, 989
Rasio F. A., Ford E. B., 1996, Sci, 274, 954
Salasnich B., Girardi L., Weiss A., Chiosi C., 2000, A&A, 361, 1023
Takeda G., Rasio F. A., 2005, ApJ, 627, 1001
Tinney C. G., Butler R. P., Marcy G. W., Jones H. R. A., Penny A. J., Vogt S. S., Apps K., Henry G. W., 2001, ApJ, 551, 507
Tinney C. G., Butler R. P., Marcy G. W., Jones H. R. A., Penny A. J., McCarthy C., Carter B. D., 2002a, ApJ, 571, 528
Tinney C. G., McCarthy C., Jones H. R. A., Butler R. P., Marcy G. W., Penny A. J., 2002b, MNRAS, 332, 759

Tinney C. G., Butler R. P., Marcy G. W., Jones H. R. A., Penny A. J., McCarthy C., Carter B. D., Bond J., 2003, ApJ, 587, 423
Tinney C. G., Butler R. P., Marcy G. W., Jones H. R. A., Penny A. J., McCarthy C., Carter B. D., Fischer D., 2005, ApJ, 623, 1171
Tinney C. G., Butler R. P., Marcy G. W., Jones H. R. A., Laughlin G., Carter B. D., Bailey J., O'Toole S., 2006, ApJ, in press
Valenti J. A., Fischer D. A., 2005, ApJS, 159, 141
Vogt S. S., Marcy G. W., Butler R. P., Apps K., 2000, ApJ, 536, 902
Vogt S. S., Butler R. P., Marcy G. W., Fischer D. A., Henry G., Laughlin G., Wright J. T., Johnson J. A., 2005, ApJ, 632, 638
Wright J., 2005, PASP, 117, 657

This paper has been typeset from a TEX/LATEX file prepared by the author.